

1 **Morphotectonic analysis by coupling a digital terrain model (DEM), radar data (Sentinel-1C)** 2 **and field data from the Eastern part of the Ouaddaï massif (Eastern Chad)**

3 **Summary**

4 The study area lies between latitudes 13°15' and 13°45' North and between longitudes 21°24' and
5 22°2' East. Administratively, it is located in the department of Asougha, province of Ouaddai. The
6 aim of this work was to carry out a morphotectonic analysis by coupling a digital terrain model, radar
7 data and field data. We used SRTM images, Sentinel 1-C radar and field campaigns. The satellite
8 images were analysed using cartographic software (ArcGIS, SNAP, Geomatica PC, RockWork, Global
9 Mapper, Surfer) and Stéronet. Observations from the 3D map were used to divide the study area into
10 three morphological units: Unit I, the lowest (altitude < 700m) where the watercourses are located; it
11 is made up of plains and valleys. Unit II, the largest, has a medium to high altitude (700-900m). This
12 geomorphological unit is made up of hills and plateaux; and Unit III is that whose altitude is > 900m.
13 This unit is made up of circumscribed hills and mountain ranges. The lineaments obtained from
14 Sentinel -C radar gave two main fracture directions: ESE-WNW and SE-NW. Field data provided the
15 lithological type, mainly granitoids. These granitoids are fractured almost everywhere in the study
16 area. These fractures follow the directions of their host rocks.

17 **Keywords:** Ouaddaï Massif, geological mapping, Lineament, Teledetection, Morphotectonics, radar

18 **Introduction**

19 Chad is part of the Central African orogenic belt, formed during the Neoproterozoic (Isseini, 2011);
20 (Bessoles, B. & Trompette, 1980). This orogenic belt remains the last tectonic event. The result of this
21 event is the formation of five major mountain ranges of Pan-African age, with a mainly granitic
22 basement interspersed with metamorphic formations (Kusnir, 1995). Alongside this basement are
23 volcanics and surface and groundwater resources. The basement is covered by overburden formations
24 (approximately 85% of Chad's total surface area) made up of two major sedimentary basins: the Erdis
25 basin in the north, which accounts for most of the surface area, and the Lake Chad basin, located
26 throughout the southern and central parts of the country (Schneider-J.L and Wolff, 1992; B.R.G.M,
27 2010b). Basement zones and sedimentary basins are rich in mineral resources (Chaussier, 1970;
28 B.R.G.M, 2010a; World bank group, 2023).

29 In this work, we review the literature on basement zones and their associated mineralization.

30 **1- Geological context**

31 Studies into the geology of Chad began in the colonial years (around 1900). Research increased after
32 1945. We might mention the work of Garde, 1911 on the Kanem; Tiho, 1913; Lacroix, 1919 on the
33 Bourkou Ennedi Tibesti; Cartier, Grossard, Fenayer and Fritel (1924-1925) on the Ouadda; Babet,

34 1940 on the Chari-Baguirmi; Van Aubel, 1942 on the Mayo-Kebbi. Unfortunately, these data are not
35 currently available in the archives. Work intensified around 1990, leading to the production of several
36 maps (sheets) by the Central African Mining and Geology Directorate, the Bureau de Recherche
37 Géologique et Minière (B.R.G.M) and the Institut Equatorial de Recherches Géologiques et Minières.
38 These include: (Bessoles, B. & Trompette, 1980; Chaussier, 1970; Gsell, J. and Sonnet, 1962; Gsell J
39 and Sonnet J., 1960; J, 1960; Mestraud, 1964; Pias, 1964; Wolff, 1964). Most of these offices have
40 carried out reconnaissance mapping of the various geological formations in Chad. On the basis of
41 these data, the lithostratigraphy of the geological formations of Chad can be divided into:
42 neoproterozoic granitoids, crystallophyll formations, paleozoic cover formations or sediments and
43 volcanics (Wolff, 1964).

44 Following this work, further work was carried out within the framework of international correlation on
45 stratigraphy or lithostratigraphy ((Kasser, 1995); (Penaye et al., 2006). This work led to the definition
46 and identification of the major lithological structures in the Mayo-kebbi massif, the Tibesti massif to
47 the north, the Ouaddaï massif to the east, the central massif, which extends the Ouaddaï massif to the
48 west, and the Mbaibokoum massif to the south (Kasser, 1995).

49 More recent work has been carried out, especially in the context of training for trainers. Examples
50 include work carried out in the Mayo-kebbi massif (Mbaguedje, 2015); (Isseini, 2011); (Doumnang,
51 2006); and in the Mbaibokoum massif (Mbaitoudji, 1984). Other more recent work has been carried
52 out as part of university studies or mining research. These include work carried out in the Tibesti
53 massif (Doumnang et al., 2024); in the Ouaddaï massif (Djerossem Nenadji, 2018; Djerossem et al.,
54 2020, 2024; Malik et al., 2024); (Hingue et al., 2024, 2025); (Malik et al., 2024); (De Wit et al., 2021);
55 or in the Central massif (Shellnutt et al., 2017, 2018, 2020). Most of these studies describe the
56 crystalline massifs of Chad as being mainly granitic.

57 The Ouaddaï massif is located in the southern part of the metacraton (Abdelsalam et al., 2002, 1998,
58 2011; Abdelsalam & Stern, 1996; Elsheikh et al., 2011; Ibinoof et al., 2016, 2021; Liégeois et al.,
59 2013; Stern & Abdelsalam, 1998). It has the shape of a plateau and covers more than 500 km². They
60 outcrop from the border with the Tibesti massif, mainly in its southern part (to the north, the Ennedi).
61 To the east, it extends into Darfur in Sudan. In the west, the Ouaddaï massif is bordered by the Central
62 massif (Schneider, 2001).

63 In lithostratigraphic terms, the Ouaddaï massif is mainly granitic. However, in its southern part,
64 metamorphic formations outcrop in abundance (Gsell J and Sonnet J., 1960; Gsell, J. and Sonnet,
65 1962; Pias, 1964; Wolff, 1964; Kusnir, 1989, 1995).

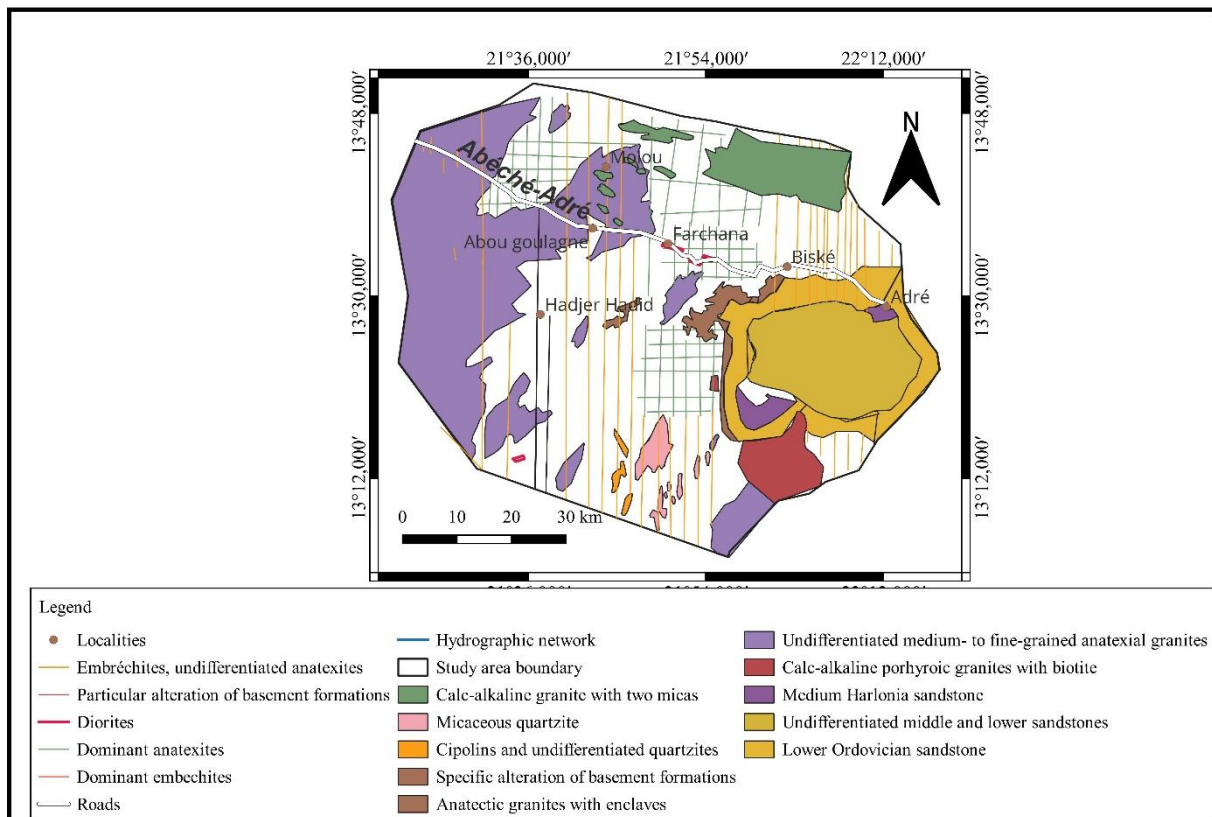
66 On the lithostructural basis, (Gsell J and Sonnet J., 1960; Gsell, J. and Sonnet, 1962) describe the
67 Ouaddaï massif as : (i) metasedimentary and metavolcanic rocks (quartzite schist, marble, cipolin,
68 migmatite); (ii) rocks with little or no metamorphism (migmatite, anatexis granodiorite, anatexis

69 granite); (iii) post-tectonic plutonic formations (calc-alkaline granite with two micas, alkaline granite,
70 porphyroid calc-alkaline granites with biotite and amphibole, granulites, aplitic granites, microdiorites,
71 syenites, diorites, microgranites, basalts); (iv) eruptive rocks and various plutonic rocks of
72 intermediate to felsic composition, forming plutons and veins intersecting the metamorphic rocks (Fig.
73 1).

74 The work of (Kusnir, 1995) illustrates that the Ouaddaï massif is purely granitic and migmatitic. The
75 metamorphic rocks identified consist of : (1) graphitic schists associated with micaceous quartzites
76 and amphibolites, located near Waya Waya, to the north-west of Guéréda; (2) banded ferruginous
77 quartzites (Hadjer Hadid to the south-west of Adré); (3) highly bedded fine-grained amphibole
78 gneisses forming elongated reliefs in a migmatitic zone (about 50 km to the north-east of Iriba) ; (4)
79 migmatites and embréchites, which form the main formations in the region near the Sudanese border;
80 (6) to the west of Mourah, cordierite and sillimanite anatexites appear in a diffuse zone within the
81 migmatitic granite; (7) meta-ultrabasites, which are less rich and include pyroxenites, which form
82 numerous outcrops between Adré and Am Leiouna. Massive amphibolites outcrop in several places (to
83 the north and north-west of Guereda, at the foot of the Modoina sandstone cliff). More recently, the
84 geological formations to the east of the Ouaddai massif have been mapped as : (1) migmatites, on the
85 Hadjer-Hadid axis; Farchana-Abou goulam-Molou-Biské; (2) calc-alkaline granite around
86 Abougoulem and north of Hadjer-hadid; (3) granite around Abéché, at Molou ; (4) calc-alkaline
87 granite with porphyritic facies south-east of the village of Kadigué, around 14 km east of Molou; (5)
88 calc-alkaline granite around Abéché, west of Hadjer-hadid, at Abou goulem (B. R.G.M, 2010b);
89 (Hingue et al., 2024, 2025). All these rocks are Neoproterozoic in age. In the vicinity of Iriba, the
90 geological formations are mapped as basanites with a SiO₂ content of around 41-45%. These basanites
91 are described as an extension of the Cameroon volcanic line, located to the west and south of
92 Cameroon (F. N. Djerosse et al., 2024).

93 In the Am Zoer sector, the rocks are mainly migmatitic and more or less differentiated (SiO₂=55.8 to
94 74.70%), calc-alkaline, metaluminous to peraluminous. They are predominantly type I granites
95 (A/CNK<1.1) with the exception of mylonite and migmatite, which belong to type S granites (Pazeu,
96 2018); dated by U/Pb on zircon, the granitoids give Pan-African ages (620-585Ma (Alexis et al.,
97 2019).

98 Towards the south of the massif, metamorphic rocks outcrop very widely (Michael, 2017); (Mbaiade,
99 2023). These are metasedimentary rocks, mainly of Neoproterozoic age (amphibolites, cipolins,
100 gneisses, micaschists, micaceous quartzites, metapelites, schists and marbles), amphibolites and
101 basalts interbedded with S-type leucogranites dated at 635Ma ±3 and 612 Ma± 8 by U-Pb on zircon;
102 type-I granitoids of Pan-African age (538±5Ma on zircon), (Djerosse, 2018).



103

104 **Figure 1:** Reconnaissance geological map of the Adré sheet, scale 1:500,000, adapted from (Gsell J
 105 and Sonnet J., 1960).

106 **2- Materials and methods**

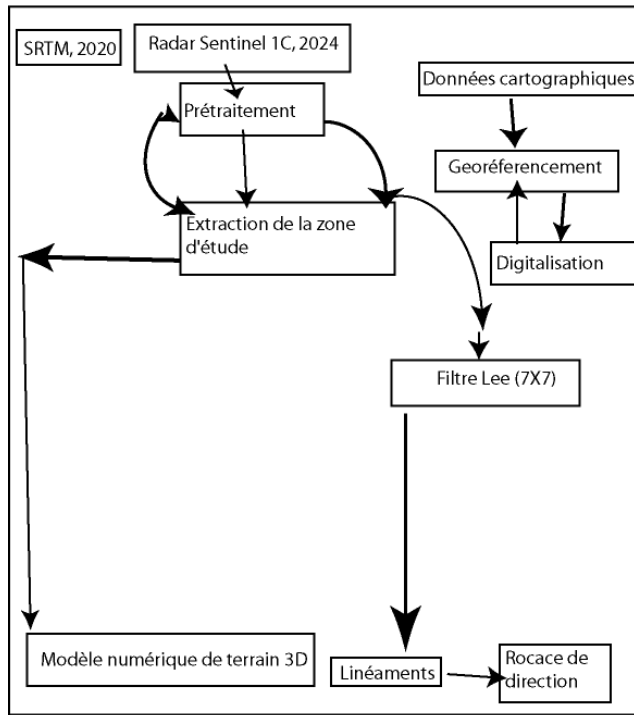
107 Four types of data are used in this article: the digital terrain model, radar (Sentinel-1C), bibliographic
 108 data and field data.

109 The digital terrain model generated from the SRTM image extracted using Global mapper and Arcgis
 110 is used to provide an overall morphological view of the massif and to generate several thematic maps
 111 (3D map, topographical profile map, etc.). The Sentinel1-C radar was used to extract the lineaments in
 112 SNAP, Geomatica PC and the steering rosette in Arcgis and Rockwoks 17. The polarisation used is
 113 called cross-polarisation (horizontal-vertical polarisation). The various steps used in this work are
 114 summarised in Figure 2.

115 The bibliographic data consisted of articles, doctoral theses, master's theses, books and reviews:

- 116 ■ a geological reconnaissance map of Adré at a scale of 1:500,000. This map was published by
 117 the Institut Equatorial des Recherches et d'Etudes Géologiques et Minières by Gsell and Sonet,
 118 1960, based on a 1/200,000 scale photograph from the Institut Géographique National. It was
 119 used to identify geological formations and locate structural features;
- 120 ■ Vector data (shapefiles). The vector data consists of the administrative boundaries of the study
 121 area, localities, watercourses and roads.

122 Terrain data consists mainly of geological structures (fracturing, foliation) and lithologies. This data
 123 was obtained during various field campaigns. This data is analysed using Stéronet software and
 124 analysed in the form of a directional rosette. This field data is used to validate the lineament and
 125 digital terrain model data and to better interpret the geological structures in the study area.



126
 127 Figure 2: image processing stages using the software

128 3- Results

129 a- Contribution of remote sensing to geological and structural mapping

130 Remote sensing has become a modern, effective tool for mapping geological and structural formations
 131 with a high degree of accuracy (Scanvic, 1986).

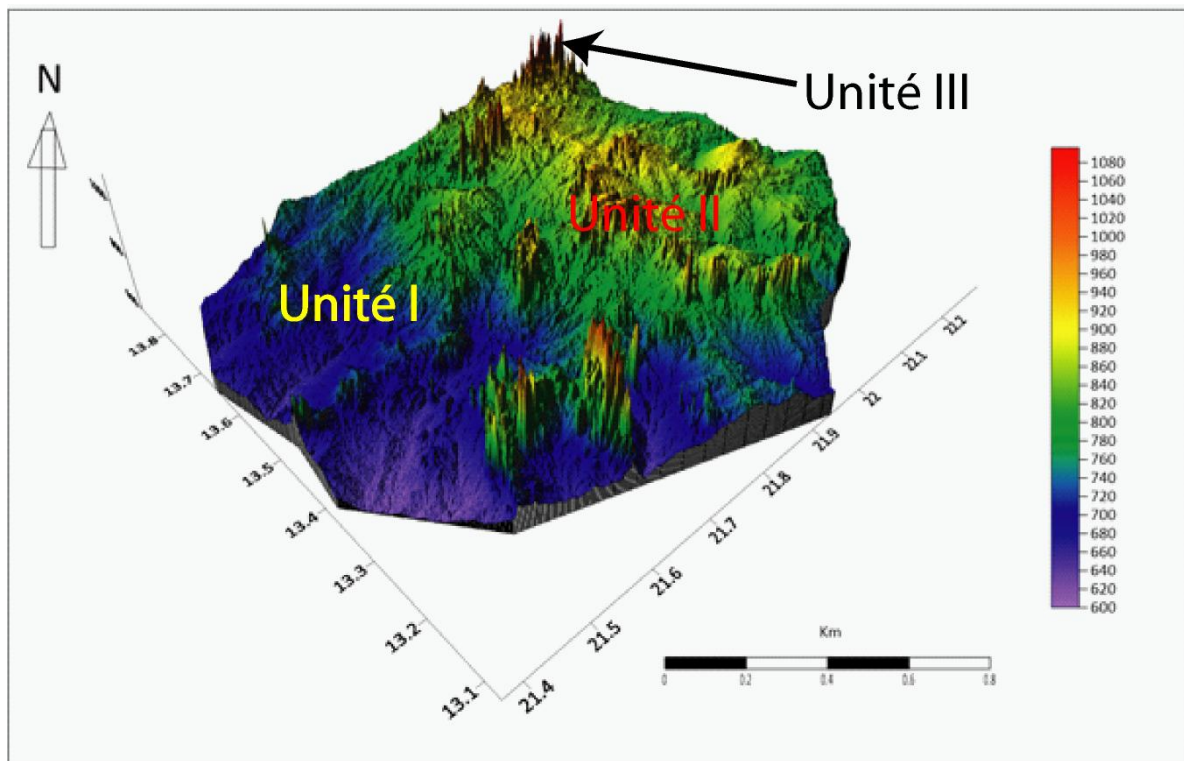
132 Orography

133 The orography of the study area is divided into four geomorphological units (units I, II and III).

134 Unit I comprises the lowest relief. It includes landforms at altitudes of $\leq 700\text{m}$ (Fig.3). It corresponds
 135 to the Ouadi Hamra depression and isolated flood plains in several places.

136 Unit (II) consists of the intermediate relief (700-900 m). This is the largest geomorphological unit. It
 137 comprises moderate to high relief. The slopes in this unit are moderate to steep (Fig. 4).

138 Unit (III) has an altitude $>900\text{m}$. It characterises the mountains to the east of Abougoulem, to the north
 139 of Hadjer-hadid and to the north-east of Molou. It has steep slopes (Fig.4).



140

141 **Figure 3:** 3D digital terrain model.

142

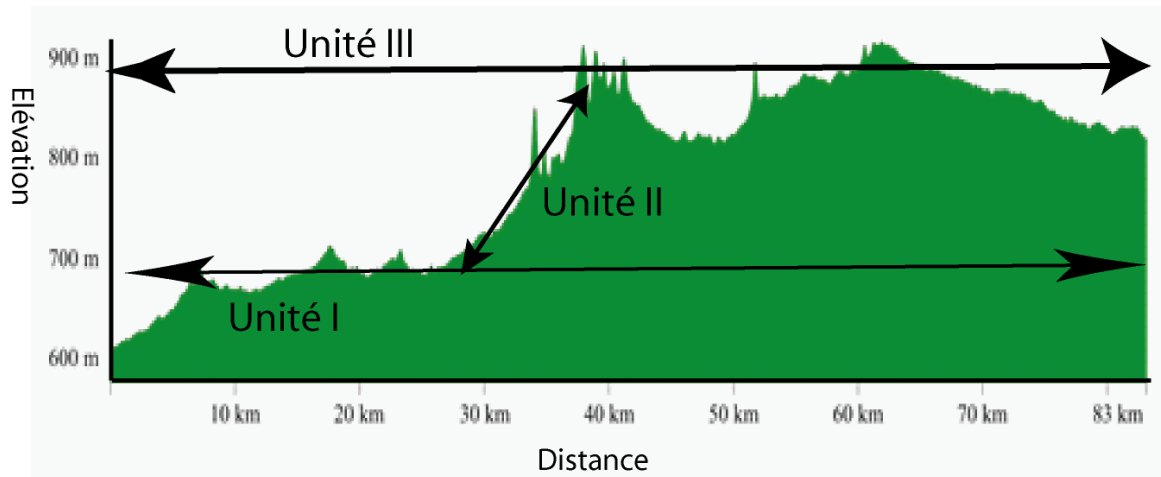
Relief typology

143 The orographic units (I) are those that drain the watercourses. They are located mainly to the north-
 144 east and south of the study area. They follow a NE-SW alignment. This unit is controlled by the
 145 Ouaddaï Hamra valley and the Bitéa streams, a tributary of the Batha (Fig. 4).

146 Geomorphological Unit II consists of hills forming mountain ranges from the north of the town of
 147 Hadjer-hadid to the south of the village of Abougoulem. This range is oriented SW-NE. Other
 148 mountain ranges can be seen to the north of the village of Molou, and to the east of the town of
 149 Farchana, specifically to the west of Biské, where it forms hills in several places.

150 Unit III is the largest, and is dominated by medium-altitude hills (Hadjer-hadid

151 Unit IV corresponds to the high altitude areas. It is defined by hills oriented SW-NE.

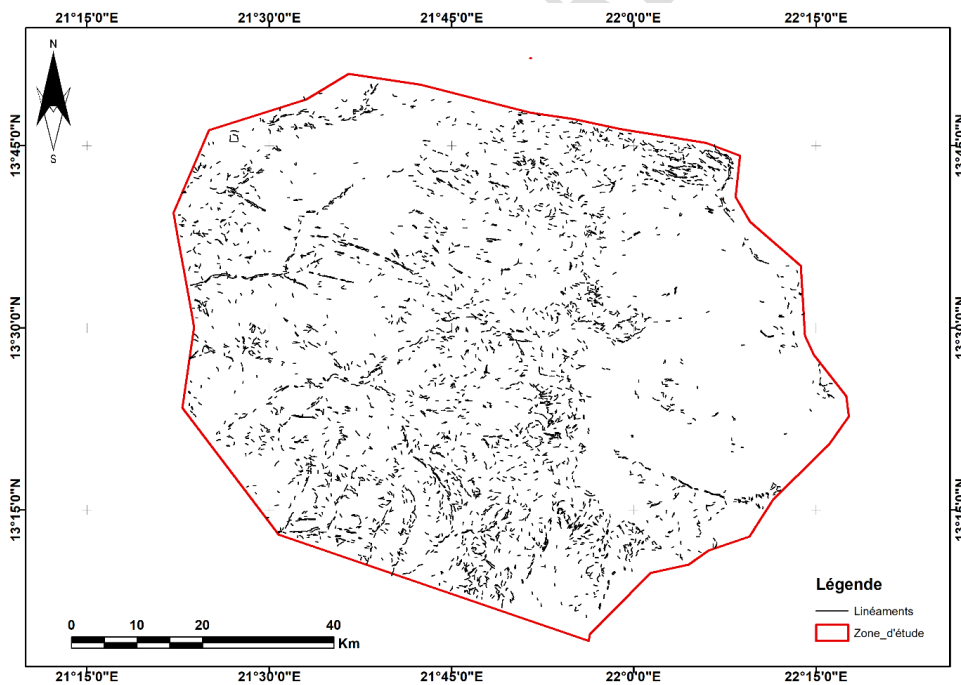


152

153 Figure 4: Topographical profile showing the different altitudes and slopes of the study area

154 **Lineament mapping**

155 Lineaments symbolise linear geological objects, arrays of geological objects (faults, joints, schistosity)
 156 that are fairly close together, geomorphological discontinuities, (Faure, 2001); (Théodore et al., 2012).
 157 These are structural faults of variable length (Faure, 2001); (Richards, 2000). The lineaments
 158 extracted from Sentinel 1-C radar were used to produce the lineament map. A total of 1096 lineaments
 159 were detected and extracted (Fig.5). They are unevenly

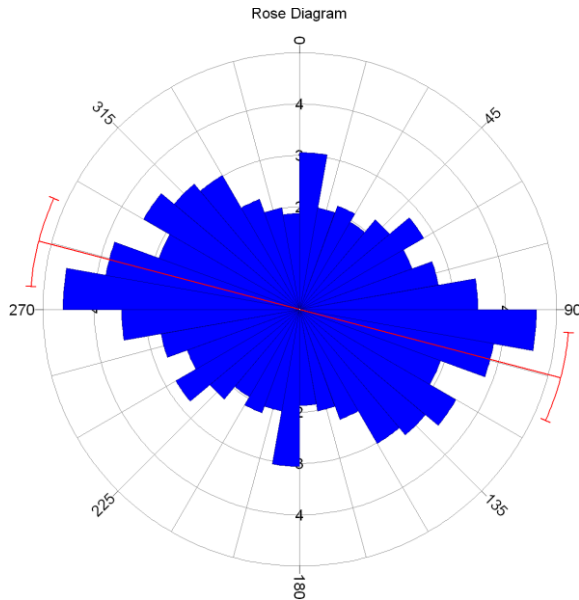


160

161 **Figure 5:** Lineament map extracted from Sentinel -1C RADAR images.

162 Directional rosette

163 The directional rosette shows a spread of lineaments in all directions (Fig. 6). However, certain
164 lineament directions stand out. These are ESE-WNW (90° to 115°), SE-NW (45° to 65°), ESE-WNW
165 and SSE-NNW (165° to 180°). Two of these directions are the main ones. These are: the SE-NW
166 direction (115° to 160°), and the ESE-WNW direction (90° to 115°) and (135° to 160°).



167

168 Figure 6: Directional rosette extracted from Sentinel-1C Radar images

169 The density of lineaments is mainly located in geomorphological units III and IV (to the south-west,
170 south-east and north of the study area. to the north-east and south of the study area. They are oriented
171 parallel to the hydrographic network and the relief. This orientation would suggest a tectonic
172 (geological) origin.

173 **b- Field data contribution**

174 **Lithology**

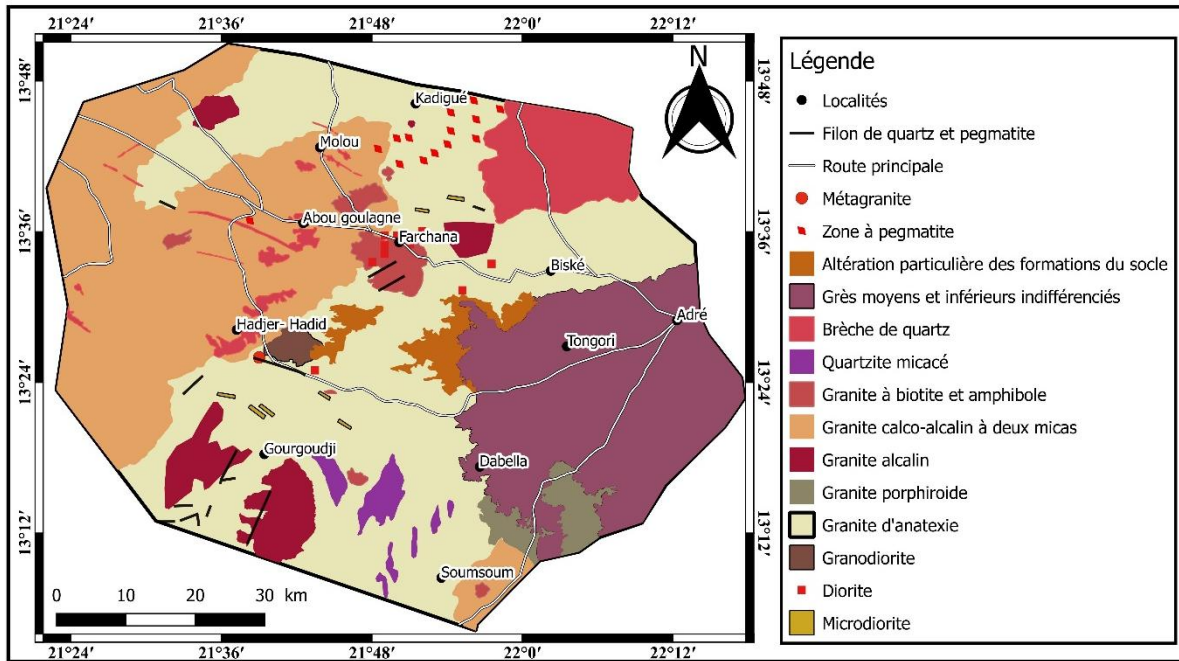
175 On a landscape scale, the geological formations to the east of the Ouaddai massif (Adré group) outcrop
176 as slabs, blocks and domes, or even mountain ranges. At the outcrop and rock scale, they are arranged
177 metrically, decametrically and even kilometre-wise (Fig. 7).



178

179 **Figure 7:** Photograph of the formations in the study area. a) Panoramic view of the diorites at
180 Farchana; b) Blocky outcrop of the granodiorites at Hadjer-hadid; c) Foliation in the granodiorites at
181 Hadjer-hadid; and d) Fracturing of the alkaline granites at Farchana.

182 The lithology of the study area consists purely of granitoids (biotite and amphibole granite, alkaline
183 granite, granodiorite, diorite, anatexis granite).

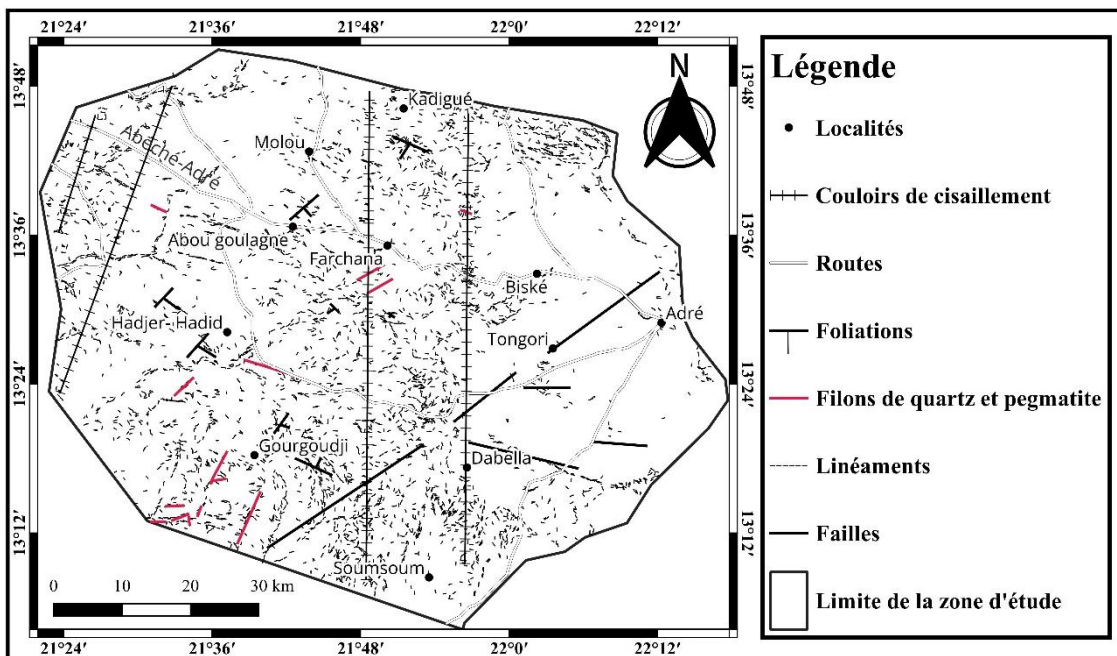


184

185 **Figure 8:** Segment of the geological map of the eastern Ouaddaï massif

186 **Tectonics**

187 The study area is made up of rocks with little or no deformation. Nevertheless, a number of structures
 188 have been identified and described.



189

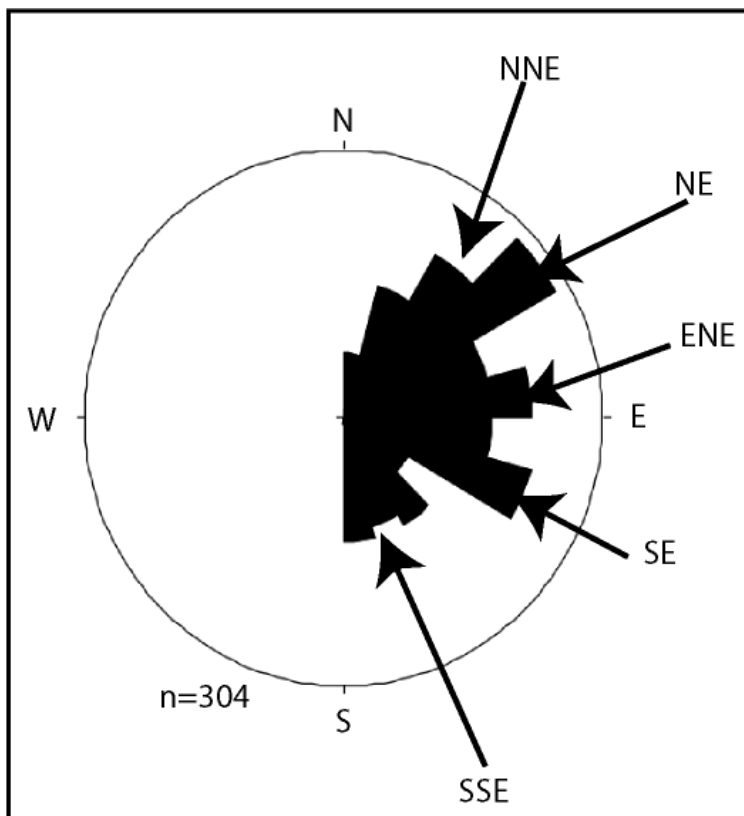
190 **Figure 9:** Structural segment of the Eastern Ouaddaï massif.

191

192 The foliation observed is magmatic (Fig. 9). This foliation is observed in granodiorites, biotite and
193 amphibole granites and alkaline granites. This is the first phase of deformation observed in the study
194 area.

195 Veins are found throughout the study area. Pegmatite veins are found throughout the lithologies
196 (Fig.9). They are mapped in abundance in the kadigué anatexis granites to the north-east of Molou,
197 where they form SW-NE trending foci.

198 All the fracturing data thus obtained were used to produce the directional rosette (Fig.10). There are
199 two main directions in this rosette: NE-SW and ESE-WNW.



200
201 Figure 10: Directional rosette of fractures in the study area.

202 4- Discussion

203 The topography of the study area is a plateau with a summit altitude of 110m. This altitude
204 corresponds to the mountain ranges observed to the north-east of Molou and to the north of Hadjer
205 Hadid.

206 a- Data control and validation

207 The control and validation of the lineament data enables the lineament data obtained to be validated
208 against that obtained from the literature and field data (Scanvic, 1986).

209 **b- Checking existing tectonic data in the study area**

210 The lineaments mapped by Radar Sentinel 1-C yielded two main fracturing directions: ESE-WNW
211 and SE-NW. These fracturing directions were also obtained by (Oussama, 2023); (Al-Djazouli et al.,
212 2019). The geological map drawn up by (Gsell J and Sonnet J., 1960) (Schneider, 2001) also gives a
213 similar fracturing direction. This direction corresponds to the main direction of the Precambrian
214 basement of the Ouaddaï massif (B.R.G.M, 2010b; World bank group, 2023).

215 **c- Checking DTM data against field data**

216 The 3D DTM map obtained from the SRTM images was used to divide the morphology of the study
217 area into map units: valleys, flat areas and hills (units I, II and III). On the ground, in the low-lying
218 areas (unit I), the diorites are widely mapped. They follow the course of watercourses. Units II and
219 III, mapped in the 3D DTM map as high-altitude areas, are mapped on the ground as circumscribed
220 hills and mountain ranges with altitudes > 110m. These units are mapped precisely to the north-east of
221 Molou and to the north of Hadjer-hadid. The hills are described as consisting mainly of biotite and
222 amphibole granites, alkaline granites, anatexis granites, metagranites, quartz breccias and
223 granodiorites. These results are confirmed in the work carried out by (Hingue et al., 2024, 2025).

224 **Checking lineaments against field data**

225 The validation of lineament data with that obtained in the field enables the physical recognition of
226 lineaments mapped in the field, especially those of great importance in geology such as faults and
227 shears. This technique is the most appropriate method for recognising lineaments. Over 300 fracture
228 planes are measured in the field. The directional rosette obtained gave two main directions: ESE-
229 WSW or N115°-135° and NE-SW or N45-70°. These latter directions are the same as those obtained
230 from the Sentinel 1-C radar. This result corroborates those of (Hingue et al., 2025).

231 **Conclusion**

232 The morphotectonic study coupled with the DTM and radar data yielded three geomorphological units
233 ranging from valleys to circumscribed hills. The lineaments obtained from Sentinel 1-C radar are those
234 of geological origin and are oriented ESE-WNW and SE-NW. These directions also correspond to
235 the direction of the different lithologies in the study area and follow the watercourse corridors. The
236 field data thus obtained has enabled us to validate the various maps obtained from the radar images
237 and the digital terrain model. It is now possible to map the geological structures using the radar digital
238 terrain model and simply validate them with the field data.

239 **Reference**

240 Abdelsalam, G., M., Liégeois, Paul, J., Stern, & J., R. (2002). The Saharan Metacraton. *Journal of*
241 *African Earth Sciences*, 34(3–4), 119–136. [https://doi.org/10.1016/S0899-5362\(02\)00013-1](https://doi.org/10.1016/S0899-5362(02)00013-1)

- 242 Abdelsalam, M. G., Gao, S. S., & Liégeois, J. P. (2011). Upper mantle structure of the Saharan
 243 Metacraton. *Journal of African Earth Sciences*, 60(5), 328–336.
 244 <https://doi.org/10.1016/J.JAFREARSCI.2011.03.009>
- 245 Abdelsalam, M. G., & Stern, R. J. (1996). Mapping Precambrian structures in the Sahara Desert with
 246 SIR-C/X-SAR radar: The Neoproterozoic Kerf Suture, NE Sudan. *Journal of Geophysical*
 247 *Research: Planets*, 101(E10), 23063–23076. <https://doi.org/10.1029/96JE01391>
- 248 Abdelsalam, M. G., Stern, R. J., Copeland, P., Elfaki, E. M., Elhur, B., & Ibrahim, F. M. (1998). The
 249 Neoproterozoic Kerf Suture in Ne Sudan: Sinistral Transpression Along the Eastern Margin of
 250 West Gondwana. *Https://Doi.Org/10.1086/516012*, 106(2), 133–147.
 251 <https://doi.org/10.1086/516012>
- 252 Al-Djazouli, M. O., Elmorabiti, K., Zoheir, B., Rahimi, A., & Amellah, O. (2019). Use of Landsat-8
 253 OLI data for delineating fracture systems in subsoil regions: implications for groundwater
 254 prospection in the Waddai area, eastern Chad. *Arabian Journal of Geosciences*, 12(7), 1–15.
 255 <https://doi.org/10.1007/S12517-019-4354-8/METRICS>
- 256 Alexis, Plunder, Jérémie, & Melleton, Matthieu Chevillard, Guillaume Vic, I Ousman Al-Gadam, et
 257 al. . (2019). Tectonometamorphic evolution of the North Ouaddaï Massif (Am Zoer area, E.
 258 Chad). *Hal-02329009*, 2.
- 259 B.R.G.M. (2010a). *Carte de favorabilité géologique à la présence d'indices métalliques (Au - U - Cu*
 260 *- Pb - Zn - W - Sn). Echelle: 1/1500 000. Planche 8.*
- 261 B.R.G.M. (2010b). *Carte des formations géologiques. Echelle 1/1500 000. Planche 1.*
- 262 Bessoles, B. & Trompette, R. (1980). *La chaîne panafricaine. Zone mobile d'Afrique centrale (partie*
 263 *sud) et zone soudanaise. Mémoire du Bureau de Recherches Géologiques et Minières, Orléans.*
- 264 Chaussier, B.J., 1970. Carte minérale du Tchad. B.R.G.M. 2^e ed. 82p
- 265 De Wit, M. J., Bowring, S., Buchwaldt, R., Dudas, F., Macphee, D., Tagne-Kamga, G., Dunn, N.,
 266 Salet, A. M., & Nambatingar, D. (2021). Geochemical reconnaissance of the guéra and ouaddaï
 267 massifs in chad: Evolution of proterozoic crust in the central sahara shield. *South African Journal*
 268 *of Geology*, 124(2), 353–382. <https://doi.org/10.25131/SAJG.124.0048>
- 269 Djerossef, F., Berger, J., Vanderhaeghe, O., Isseini, M., Ganne, J., & Zeh, A. (2020). Neoproterozoic
 270 magmatic evolution of the southern Ouaddaï Massif (Chad). *Bulletin de La Société Géologique*
 271 *de France*, 191(1), 34. <https://doi.org/10.1051/BSGF/2020032>
- 272 Djerossef, F. N., Mbassa, B. J., Vanderhaeghe, O., & Gregoire, M. (2024). Comptes Rendus
 273 Géoscience. *Comptes Rendus. Géoscience. Académie des Sciences de La Planète*, 356(G1), 231–248.
 274 <https://doi.org/10.5802/crgeos.282>

- 275 Djerosseem Nenadji, F., 2018. Croissance et remobilisation crustales au Pan-Africain dans le sud du
276 massif du Ouaddaï (Tchad). Thèse doct.Univ.Toulouse.303p
- 277 Djerosseem, Nenadji, F., Rirabé, N., Ronang Baïssema, G., Ngarena Klamadji, M., & Hisseine Malik,
278 M. (2024). Lineament and Lithological Mapping of Meta-Sediments and Granitoids of Goz-
279 Beïda (Eastern Chad) Based on Semi-Automatic Processing of Landsat 8 Oli/Tirs Images.
280 *Journal of Geosciences and Geomatics*, 12(4), 80–86. <https://doi.org/10.12691/JGG-12-4-1>
- 281 Doumnang, Claude, M. J., Diondoh, M., Tekoum, L., & Rochette, P. (2024). Teleanalysis, structural
282 mapping of t, geological and he southern zone of the Ttibesti metallogenic province (NortherN
283 Chad). *International Journal of Applied Science and Research*, VOLUME 7(ISSUE 6
284 NOVEMBER – DECEMBER), 133–147.
- 285 Doumnang, J.-C. (2006). *Géologie des formations néoprotérozoïques du Mayo Kebbi (Sud-Ouest du*
286 *Tchad) : apport de la pétrologie et de la géochimie : implications sur la géodynamique au*
287 *Panafricain / Theses.fr*. Orléans.
- 288 Elsheikh, A., Abdelsalam, M. G., & Mickus, K. (2011). Geology and geophysics of the West Nubian
289 Paleolake and the Northern Darfur Megalake (WNPL–NDML): Implication for groundwater
290 resources in Darfur, northwestern Sudan. *Journal of African Earth Sciences*, 61(1), 82–93.
291 <https://doi.org/10.1016/J.JAFREARSCI.2011.05.004>
- 292 Faure, S. (2001). Analyse des linéaments géophysiques en relation avec les minéralisations en or et
293 métaux de base de l’Abitibi. In *Rapport Projet CONSOREM (Vols. 2000-03A)*.
- 294 Gsell, J. and Sonnet, J. (1962). *Prospection de re-connaissance sur la coupure de Niéré (feuille de*
295 *Niéré N° ND 34 NE 0.80-E.8*.
- 296 Gsell J and Sonnet J., 1960. (1960). Carte géologique de reconnaissance au 1/500.000 et notice
297 explicative sur la feuille Adre. Brazzaville. *BRGM*, 42.
- 298 Hingue, N. V., Diondoh, M., Mbaigane, D., Claude, J., Lutian, A., Mbaïade, B., & Mbaïhoudou, D.
299 (2025). *Research article geological and structural mapping of the ouaddaï massif using landsat*
300 *and radar data*.
- 301 Hingue, N. V., Mbaigané, J. C. D., Diondoh, M., & Mbaïhoudou, D. (2024). Petrography and
302 Geochemistry of the Farchana-Hadjerhadid Granitoids (Ouaddaï Massif, Eastern Chad).
303 *European Journal of Environment and Earth Sciences*, 5(4), 8–15.
304 <https://doi.org/10.24018/EJGEO.2024.5.4.473>
- 305 Ibinoof, A., M., Bumby, A. J., Liégeois, J.-P., Grantham, G. H., Armstrong, R., & Le Roux, P. (2021).
306 *The Boundary Between the Saharan Metacraton and the Arabian Nubian Shield: Insight from*
307 *Ediacaran Shoshonitic Granites of the Nuba Mountains (Sudan): U–Pb SHRIMP Zircon Dating*,

- 308 *Geochemistry and Sr–Nd Isotope Constraints*. 39–62. [https://doi.org/10.1007/978-3-030-72995-](https://doi.org/10.1007/978-3-030-72995-0_2)
309 [0_2](https://doi.org/10.1007/978-3-030-72995-0_2)
- 310 Ibinoof, M. A., Bumby, A. J., Grantham, G. H., Abdelrahman, E. M., Eriksson, P. G., & le Roux, P. J.
311 (2016). Geology, geochemistry and Sr–Nd constraints of selected metavolcanic rocks from the
312 eastern boundary of the Saharan Metacraton, southern Sudan: A possible revision of the eastern
313 boundary. *Precambrian Research*, 281, 566–584.
314 <https://doi.org/10.1016/J.PRECAMRES.2016.06.010>
- 315 Isseini, M. (2011). *Croissance et différenciation crustales au Néoprotérozoïque : exemple du domaine*
316 *panafricain du Mayo Kebbi au Sud-Ouest du Tchad* [Université Henri Poincaré - Nancy 1].
317 <https://hal.univ-lorraine.fr/tel-01746184>
- 318 Jean Pias. (1960). *Sols de la région Est du Tchad. plaines de Piedmont. massif du Ouaddai et de*
319 *l'Ennedi.*;rapport. B.R/G.M.1960.336p
- 320 Kasser, Y. M. (1995). *Evolution précambrienne de la région du Mayo Kebbi (tchad), un segment de la*
321 *chaîne pan-africaine*
322 [dohttps://bibliotheques.mnhn.fr/medias/doc/Exploitation/horizon/472164/evolution-](https://bibliotheques.mnhn.fr/medias/doc/Exploitation/horizon/472164/evolution-precambrienne-de-la-region-du-mayo-kebbi-tchad-un-segment-de-la-chaîne-pan-africaine)
323 [precambrienne-de-la-region-du-mayo-kebbi-tchad-un-segment-de-la-chaîne-pan-africaine](https://bibliotheques.mnhn.fr/medias/doc/Exploitation/horizon/472164/evolution-precambrienne-de-la-region-du-mayo-kebbi-tchad-un-segment-de-la-chaîne-pan-africaine)
- 324 Kusnir, I. (1989). *aperçu sur la géologie, les ressources minérales et en eau du Tchad.*
- 325 Kusnir, I. (1995). *Géologie, ressources minérales et ressources en eau du Tchad ; Travaux.* centre
326 national de recherche.217P
- 327 Liégeois, Jean, P., Abdelsalam, G., M., Ennih, N., & Ouabadi, A. (2013). Metacraton: Nature, genesis
328 and behavior. *Gondwana Research*, 23(1), 220–237. <https://doi.org/10.1016/J.GR.2012.02.016>
- 329 Liégeois, Paul, J., Abdelsalam, M. G., Ennih, N., & Ouabadi, A. (2013). Metacraton: Nature, genesis
330 and behavior. *Gondwana Research*, 23(1), 220–237. <https://doi.org/10.1016/J.GR.2012.02.016>
- 331 Malik, M. H., NgonNgon, G. F., Vishiti, A., Mayer, A.-S. A., Isseini, M., Djerossem, F., & Al-Gadam,
332 I. O. (2024). Petrography and mineral microchemical signature of lode gold mineralization in
333 Goz-Beida, southern Ouaddaï massif, eastern Chad. *Arabian Journal of Geosciences* 2024 17:7,
334 17(7), 1–19. <https://doi.org/10.1007/S12517-024-12011-5>
- 335 Mbaguedje, D. (2015). *Métallogénie de l'or et de l'uranium dans le cadre de la croissance et de la*
336 *différenciation de la croûte au Néoprotérozoïque : exemple du massif du Mayo-Kebbi (Tchad)*
337 *dans la Ceinture Orogénique d'Afrique Centrale* [Université de Lorraine]. [https://hal.univ-](https://hal.univ-lorraine.fr/tel-01751338)
338 [lorraine.fr/tel-01751338](https://hal.univ-lorraine.fr/tel-01751338)
- 339 Mbaiade, B. (2023). *Etude géologique de la localité de Goz-Beida (région est du Tchad) : apport de la*

- 340 *téledétection, la pétrographie et la structurale*.Mém.mast.Univ.N'gaoundéré.90p
- 341 Mbaitoudji, M. . (1984). *Lois de répartition, hypothèse de pronostics et méthodologie de la recherche*
342 *des gisements de minéraux utiles solides dans le territoire de la République du Tchad.rapport.*
343 *14p*
- 344 Mestraud, J. P. (1964). Carte géologique de la République Centrafricaine à l'échelle du 1/1.500.000.
345 *BRGM.*
- 346 Michael, G. houahdibe. (2017). *Contribution à l'étude pétrographique et structurale du secteur Nord*
347 *de Goz-Beïda (Massif du Ouaddaï-Tchad).Mém.mast.univ.N'gaoundéré.85p*
- 348 Oussama, M. A. T. (2023). *Etudes pétrographique et structurale des formations magmatiques et*
349 *métamorphiques du massif du Ouaddaï (Axe Abéché – Adré).Mém.Mast.univ.N'djaména.46p*
- 350 Pazeu, Y. G. (2018). *Caractéristiques, pétrographiques, structurales et géochimiques du socle*
351 *précambrien de la localité d'Am Zoer : massif du Ouaddaï (Est du*
352 *TCHAD).Mém.Mast.Univ.N'gaoundéré.89p*
- 353 Penaye, J., Kröner, A., Toteu, S. F., Van Schmus, W. R., & Doumnang, J. C. (2006). Evolution of the
354 Mayo Kebbi region as revealed by zircon dating: An early (ca. 740 Ma) Pan-African magmatic
355 arc in southwestern Chad. *Journal of African Earth Sciences*, 44(4–5), 530–542.
356 <https://doi.org/10.1016/J.JAFREARSCI.2005.11.018>
- 357 Richards, J. P. (2000). Lineaments Revisited. *Society of Economic Geologists*, 42, 1–20.
358 <https://doi.org/10.5382/SEGNEWS.2000-42.FEA>
- 359 Scanvic, J. Y. (1986). *Téledétection aérospatiale et informations géologiques. Manuels et Méthodes.*
360 *Éditions (Éditions 2d).*
- 361 Schneider, J. L. (2001). *Géologie, Archéologie, Hydrogéologie de la République du Tchad.. Carte de*
362 *valorisation des eaux souterraines de la République du Tchad, 1/1500000, Direction de*
363 *l'hydraulique, N'djamena.* <https://www.sci epub.com/reference/372321>
- 364 SchneiderJ.L, & Wolff, J. . (1992). Carte géologique et cartes hydrogéologiques à 1/1 500 000 de la
365 République du Tchad. Mémoire explicatif. In *Documents - B.R.G.M.* Bureau de recherches
366 géologiques et minières.
- 367 Shellnutt, GregoryJ., Pham, N. H. T., Yeh, M. W., & Lee, T. Y. (2020). Two series of Ediacaran
368 collision-related granites in the Guéra Massif, South-Central Chad: Tectonomagmatic constraints
369 on the terminal collision of the eastern Central African Orogenic Belt. *Precambrian Research*,
370 347, 105823. <https://doi.org/10.1016/J.PRECAMRES.2020.105823>
- 371 Shellnutt, J. G., Pham, N. H. T., Denyszyn, S. W., Yeh, M. W., & Lee, T. Y. (2017). Timing of

372 collisional and post-collisional Pan-African Orogeny silicic magmatism in south-central Chad.
373 *Precambrian Research*, 301, 113–123. <https://doi.org/10.1016/J.PRECAMRES.2017.08.021>

374 Shellnutt, J. G., Yeh, M. W., Lee, T. Y., Iizuka, Y., Pham, N. H. T., & Yang, C. C. (2018). The origin
375 of Late Ediacaran post-collisional granites near the Chad Lineament, Saharan Metacraton, South-
376 Central Chad. *Lithos*, 304–307, 450–467. <https://doi.org/10.1016/J.LITHOS.2018.02.020>

377 Stern, R. J., & Abdelsalam, M. G. (1998). Formation of juvenile continental crust in the Arabian-
378 Nubian shield: Evidence from granitic rocks of the Nakasib suture, NE Sudan. *International*
379 *Journal of Earth Sciences*, 87(1), 150–160.

380 Théodore, Yao, K., Olivier, & Fouché-Grobla, Marie-Solange Yéi Oga, V. T. A. (2012). Extraction de
381 linéaments structuraux à partir d'images satellitaires, et estimation des biais induits, en milieu
382 desocle précambrien métamorphisé. *Teledetection*, 10 (4), pp.161-178. (hal-01948904).

383 Wolff, J. P. (1964). *Carte géologique de la République du Tchad au 1/1500000*, BRGM, Paris.

384 World bank group. (2023). *Tchad Rapport diagnostique du secteur minier*. Rapport. 131p

385